

# FATIGUE CRACK CLOSURE UNDER CYCLIC TENSION

WOLF ELBER

Institut für Festigkeit, Mülheim, Germany

**Abstract**—Results of an investigation are presented, which indicate that a fatigue crack, propagating under zero-to-tension loading may be partially or completely closed at zero load. An analysis of the stress distribution acting on the fracture surfaces shows that the local compressive stress maxima may exceed the yield stress of the material. Fractographic evidence is presented to show that crack closure may influence the shape of the striation pattern on the fracture surfaces.

## NOTATION

$P, T_1, T_2, C$	testing forces or residual resultant forces
$\epsilon, e_1, e_2, e$	testing eccentricities or residual eccentricities
$\delta, \delta_0, \delta_1$	displacements between sections
$F, \frac{d\delta}{dP}$	flexibility of the structure for any set of displacements and forces
$\sigma_{\max}$	the local peak stresses on the fracture surface over areas smaller than the width of one striation
$\sigma_{\text{nom}}$	local nominal stresses averaged over the area of at most several striations
$C_0$	compatibility factor on the micro-scale
$\Delta\sigma$	gross stress increment in one loading cycle
$\Delta K$	appropriate rise in the stress intensity factor
$\alpha$	constant associated with crack closure

## 1. INTRODUCTION

IN THE study of fatigue crack propagation, crack closure has usually only been considered to occur under compressive loads. Rice[1] has excluded the occurrence of crack closure under cyclic tension loading in the stress analysis of the crack tip. This, however, applies only to an idealized crack which is not propagating. As a consequence of the permanent tensile plastic deformation left in the wake of a fatigue crack, one should expect partial crack closure after unloading the specimen[2]. This question is studied in the present paper.

The experiments described here, show that a fatigue crack propagating under zero-to-tension loading was fully closed at zero load due to internal forces existing in the specimen. The experiments were based on the following two principles:

(1) The net internal force acting across a section in a statically indeterminate structure can be obtained by cutting the section and measuring the force system required to reverse the displacement system produced by the cut.

(2) A crack in a structural member is closed, when the stiffness of the member is the same as the stiffness of an identical uncracked member under the same load system.

The crack closure phenomenon was first observed when a partially cracked sheet specimen of the type shown in Fig. 1, was cut open in order to allow fractographic investigations of the fracture surfaces. This cutting was accompanied by deformations large enough to be observed by the naked eye. The specimen was then equipped with strain gauge targets (Fig. 1), and a force system ( $P, \epsilon$ ) was applied. The relationship between the force  $P$ , and the displacement at the edge of the specimen is shown in Fig. 2. This relationship is elastic but non-linear with a stiffness increasing with the

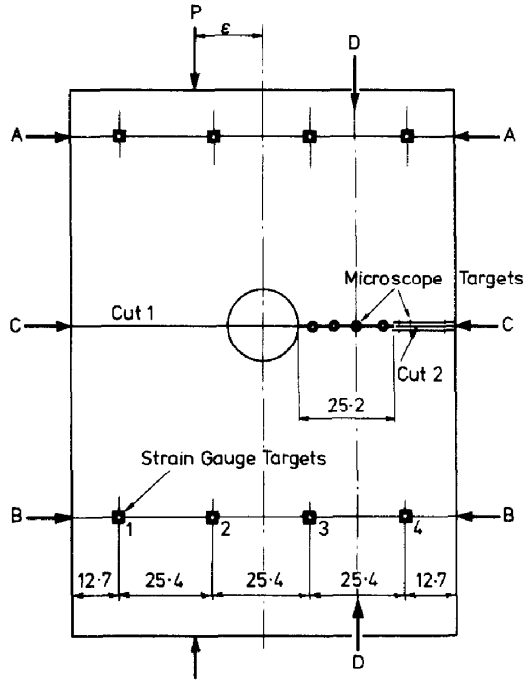


Fig. 1. Specimen configuration and instrumentation. (Clamping area removed.)

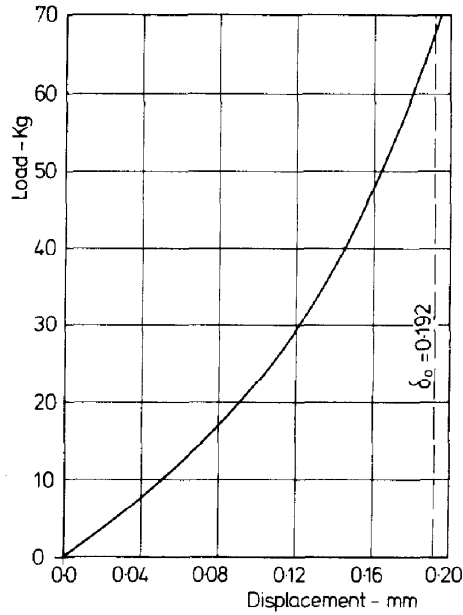


Fig. 2. Relation between testing load and edge displacement.

applied force. This immediately suggests that the system has a varying geometry, which in turn can only mean that the crack is closing. Following this preliminary experiment, a more complete analysis of the internal force system was made.

## 2. ANALYSIS OF THE INTERNAL FORCE SYSTEMS

From the preliminary results, it was concluded that the stress distribution across the critical section of the specimen must be of the form shown in Fig. 4(a). There are three regions in which compressive stresses act.

- (1) *A-B* The cracked section.
- (2) *B-C* Part of the plastic zone ahead of the crack tip.
- (3) *D-E* Part of the plastic zone on the uncracked side of the notch.

The remaining sections would be under tension.

Instead of carrying out a complete analysis of this statically indeterminate system, it is possible to treat the specimen as if it consisted of three main members each carrying a two parameter force system ( $P, \epsilon$ ), representing the net force ' $P$ ' on the section with an eccentricity ' $\epsilon$ ' from the centre of the sheet.

The force system on the uncracked side of the specimen will be labelled ( $T_1, e_1$ ), the force system acting on the crack surfaces by ( $C, e$ ) and the force system acting on the remaining portion of the cracked side of the specimen will be labelled ( $T_2, e_2$ ), see Fig. 4(a). In order to determine the tensile force systems, the section over which it acts is cut and the displacement system resulting from this cut has to be obtained as a two parameter system. It was found that the displacement system between sections *A-A* and *B-B* in Fig. 1 was linear across the specimen width when a 100 mm base length was used.

The force system ( $T_1, e_1$ ) and ( $T_2, e_2$ ) cannot both be determined from the same specimen. Therefore a series of identically cracked specimens was required.

The force system ( $C, e$ ) can be obtained from the two tensile force systems using the following equations.

$$C = T_1 + T_2$$

$$e = (T_2 \cdot e_2 - T_1 \cdot e_1) / C.$$

### *Preparation of specimens*

The material of the specimen was an aluminum alloy 65 S-T6 (composition Mg: 1.0, Si: 0.6, Cu: 0.28, Cr: 0.25) with the following static properties:  $S_u = 38 \text{ kg/mm}^2$ ,  $S_{0.2} = 37 \text{ kg/mm}^2$  and elongation 10 per cent. Dimensions of the specimens were: width 100 mm, thickness 6.35 mm, hole diameter 19 mm and crack length 25 mm, see also Fig. 1.

Two specimens were required for the determination of the force systems ( $T_1, e_1$ ), and ( $T_2, e_2$ ). They had to satisfy the following requirements:

- (1) The crack length had to be equal and approx. 25 mm in length.
- (2) The modes of failure had to be similar, being single cracks and preferably of the double shear mode type to prevent distortion during sectioning.
- (3) The load spectrum producing the cracks was required to have a minimum tension load as close as possible to zero, so that the examination in the unloaded

condition would reveal the residual stress distribution at the minimum load of the applied load spectrum.

The fatigue load adopted induced the following gross stresses in the specimen:  $S_{\max} = 10 \text{ kg/mm}^2$   $S_{\min} = 0.3 \text{ kg/mm}^2$ .

Displacements between sections *A-A* and *B-B* were measured by means of Huggenberger Tensotast equipment using the ball-point targets shown in Fig. 1.

#### *Force systems ( $T_1, e_1$ ) and ( $T_2, e_2$ )*

The first specimen was sectioned along the line marked 'Cut 1' and the displacement system  $(\delta_0, \delta_1)$  was measured. The force system  $(P, \epsilon)$  was then applied, and the eccentricity  $\epsilon$  was increased until a displacement system  $(-\delta_0, -\delta_1)$  was obtained. ( $\delta_0$  and  $\delta_1$  are the displacements at the two edges of the specimen).

This experiment was repeated using the second specimen with a cut labelled 'Cut 2', and the force system was found which would reverse the displacement system caused by Cut 2.

The resulting two force systems  $(T_1, e_1)$ ,  $(T_2, e_2)$  and the calculated force system  $(C, e)$  are shown in Fig. 4(b).

It must be noted that these force systems are only estimates of the real force systems acting in the uncut specimen, because the point of application of the force system  $(P, \epsilon)$  is not identical with the centroid of the force system  $(T_1, e_1)$  or  $(T_2, e_2)$ . However, the resulting errors are believed to be relatively small.

#### *Flexibility studies*

Since a total compressive force of 395 kg was acting across the fracture faces, the crack in the specimen is at least partially closed in the unloaded state. Further experimentation was required to ascertain whether the crack was completely or only partially closed. Microscopic observation at the specimen surface appeared to be inadequate, since at the surface the crack always appears to be open. Repolishing of the specimen could not be attempted because of the instrumentation on the surfaces.

It was therefore decided to ascertain the degree of crack closure by studying the flexibility of the specimen under the force system  $(T_1, e_1)$ , and comparing this with the flexibility of a similar specimen also sectioned along Cut 1, but containing an artificial sawcut crack instead of the fatigue crack.

For this purpose a third specimen was sectioned along Cut 1, and subjected to the force system  $(T_1, e_1)$ . The displacement between sections *AA* and *BB* was measured at the edge of the specimen in order to obtain the greatest sensitivity. This displacement at the free edge of the specimen has been labelled ' $\delta$ '.

The relation between the force  $T_1$  and the displacement  $\delta$  was found to be linear and can be expressed by the equation

$$\delta = F \cdot T_1$$

where  $F$  is a flexibility constant. This constant  $F$  was obtained for various lengths of the artificial sawcut crack in the specimen.

As a next step, specimen 1 was again subjected to the force system  $(T_1, e_1)$ , and the relation between the force  $T_1$  and the displacement  $\delta$  was established. This relation is nonlinear, although the specimen appears to behave elastically. This indicates that

there is a progressive change in the geometry of the specimen, which must be caused by the closing of the crack under the force  $T_1$ . The relation is shown graphically in Fig. 2. The dotted line indicates the displacement  $\delta_0$  required to reverse the displacement caused by the sectioning.

The cotangent of the load-displacement curve represents the flexibility of the specimen. This is given by

$$\frac{d\delta}{dT_1} = F.$$

The relation between the flexibility  $F$  and the displacement  $\delta$  was obtained from Fig. 2.

If it is assumed that the flexibility of the specimen containing the artificial crack is the same as the flexibility of Specimen 1 with the crack being open to the same length, then a relation can be established between the load  $T_1$  and the open crack is shown in Fig. 3.

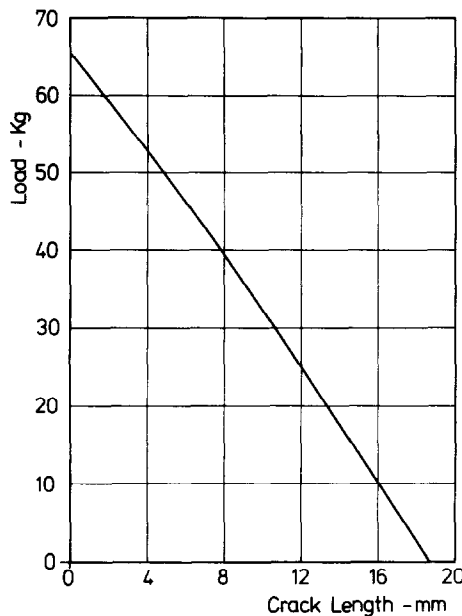


Fig. 3. Relation between testing load and length of open crack.

From this figure it can be seen that at a load of 66 kg, which is just below the load required to reverse the displacement system caused by sectioning specimen 1, the open crack length is zero. This means that in the unloaded state the crack is completely closed.

When the load  $T_1$  is zero, the open crack length is 18.5 mm, whereas the total crack length is 25.2 mm. This means that after sectioning along Cut 1 the crack still appears to be partially closed.

#### *The free shape of the fracture surfaces*

From the experiments just described, it can be concluded that the fracture surfaces are not plane, and that they are incompatible in the free state. It was possible to obtain

an estimate of the free shape of the fracture surfaces by taking further simultaneous measurements of the opening of the crack and the displacement of sections *AA* and *BB*.

Since the crack of Specimen 1 was still partially shut after sectioning along Cut 1, the remainder of the section was progressively sectioned along Cut 2 and measurements were taken of the crack opening, the displacements across the cut and the displacements between the sections *AA* and *BB*.

Using the fact that the body deformations between sections *AA* and *CC* are equal to half the difference between the relative displacements of sections *AA* and *BB* at any section *DD* (see Fig. 1) and the crack opening at section *DD*, it is possible to calculate the free shape of the fracture surfaces. Using data from a total of seven observation points along section *CC*, the free shape of the fracture surfaces can be constructed. This free shape is shown on a distorted scale in Fig. 4(c).

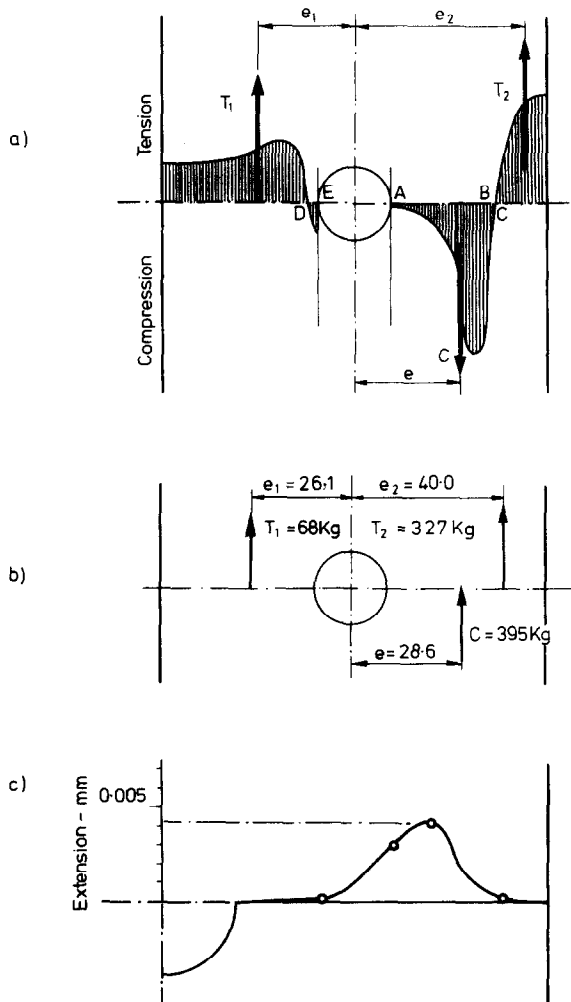


Fig. 4. (a) Assumed residual stress distribution and resultant force systems. (b) Experimentally obtained force systems. (c) Shape of the free fracture surface.

### *Estimation of crack closure stresses*

Given the free shape of the two incompatible fracture surfaces, it is possible to establish by methods of elastic analysis a stress distribution which would satisfy compatibility along the section  $CC$  at every point. It is felt, however, that the experimental techniques used in obtaining the free shape of the fracture surfaces only justify an estimate of the maximum compressive stresses acting across the fracture surfaces.

Such an estimate can be based on the force system  $(C, e)$ , using the assumption that the crack closure stresses are distributed such that they increase monotonically from zero at the original notch root to a maximum at the crack tip.

The centroid of the force  $C$  is approximately at one quarter of the crack length from the crack tip. A parabolic stress distribution would also have its centroid at that point. The maximum stress at the crack tip would be  $7.5 \text{ kg/mm}^2$ , if a parabolic distribution is assumed.

In view of the deformation of the fracture as illustrated by Fig. 4(c), it is expected that the stress will rise sharper than parabolically. Hence the value of  $7.5 \text{ kg/mm}^2$  is probably too low and a value in the order of  $10 \text{ kg/mm}^2$  seems to be more appropriate for the discussion.

### *Micro compatibility of the fracture surfaces*

A fractographic investigation of the fracture surfaces has shown that only a fraction of the surface area is capable of making contact with the opposite surface. This means that the average stresses calculated are transmitted over a reduced area. If we define a local compatibility factor ' $C_0$ ' as the ratio of load bearing area to total area, then the local peak stress  $\sigma_{\max}$  is given by

$$\sigma_{\max} = C_0 \times \sigma_{\text{nom}}$$

If we suppose that the shape of the fracture surface at the moment of formation has a shape of either the non-mating sawtooth model or the more general non-mating continually undulated surface, then during the first instant of unloading the compatibility factor would be zero. During the process of crack closure the peak local stresses are limited to a yield level, while the nominal stress  $\sigma_{\text{nom}}$  increases to the measured and calculated value. As a result, the compatibility factor must vary by either elastic or plastic deformations. Hence, the shape of the striations as formed during the crack propagation process will be changed during crack closure until sufficient compatible surface is available to carry the compressive forces.

Using an approximate yield stress of  $30 \text{ kg/mm}^2$  for the aluminum alloy under repeated hammering, and the calculated maximum nominal stress of  $10 \text{ kg/mm}^2$ , a surface compatibility of approximately one third is required.

Fractographic investigations have been carried out on the fracture surfaces. The surface shown in Fig. 5 can be interpreted to consist of a generally flat surface in which the striations represent grooves.

The area encircled and labelled (a) shows striation grooves wider than the areas (b) and (c). The degree of surface compatibility can be estimated at approximately 50 per cent, whereas in area (c) the surface compatibility approaches 100 per cent.

On the assumptions that the maximum nominal stress is  $10 \text{ kg/mm}^2$ , the yield stress at which the surface can be deformed is  $30 \text{ kg/mm}^2$ , we obtain a surface compatibility of 33 per cent, below which the surfaces must be deformed in order to carry the crack closure stresses.

Conversely, since the observations are made after the deformation process, the lowest surface compatibility found should be of the order of 33 per cent.

Systematic investigation of the fracture surfaces has shown that areas of a surface compatibility of less than 20 per cent were extremely rare and never extended over large areas.

The fractographic evidence can be used to reverse the argument in the following way. It is assumed that the flat surface features were not formed as such during the crack propagation, because this would require cleavage fracture. Hence deformations during crack closure are responsible for the flattening of the striation peaks.

### 3. CONCLUSIONS

From the results presented above we can draw the following conclusions:

- (1) The crack closure phenomenon is a direct consequence of the permanent tensile plastic deformations left in the wake of the propagating crack. These deformations make the mating fracture surfaces incompatible.
- (2) A crack in a fatigue specimen is fully open for only a part of the load cycle, even when the loading cycle is fully in tension.
- (3) The striation shape on the fracture surfaces is determined not only by the crack propagation process, but also by the crack closure stresses, when these reach load maxima above the yield stress in compression.
- (4) Under constant amplitude loading, the loading conditions at the crack tip cannot be determined solely by the stress intensity factor ( $\Delta K$ ) resulting from the whole stress increment  $\Delta\sigma$ . If the crack is fully open for a fraction ' $\alpha \times \Delta\sigma$ ' of the load cycle, then it may be possible to correlate the rate of crack propagation with  $\alpha \times \Delta K$ . If the fraction  $\alpha$  is constant with crack length and mean stress level, the fourth power relationship between  $\Delta K$  and the rate of crack propagation would not be affected.
- (5) Under variable amplitude loading, crack closure may be responsible for at least part of the interaction effects between stress levels.

Further work, both theoretical and experimental, is required to establish the influence of crack closure on the crack propagation process. The most important aspects of this are:

- (1) The determination of the 'crack opening load', that load at which contact between the fracture surfaces is broken, and at which the stress distribution at the crack tip first experiences the singularity of the theoretically sharp crack.
- (2) The determination of the 'crack closure load', that load at which contact between the fracture surfaces is established on unloading. This load should always be higher than the 'crack opening load'.
- (3) The determination of the difference between the 'crack closure load' and the subsequent 'crack opening load' as a function of the intermediate load minimum.
- (4) The determination of the rate at which the 'crack opening load' decreases, if the load cycling has been dropped below this opening level. Such low level cycling (for instance ground-to-air cycle in aeronautical fatigue) would obviously increase the crack closure stresses and would cause compressive deformations on the fracture surfaces, thus decreasing the load at which the crack will again reopen.

At the present stage, it appears that theoretical calculation of the crack closure phenomenon presents great difficulties. Hence, the data required would have to be obtained by experimental means.



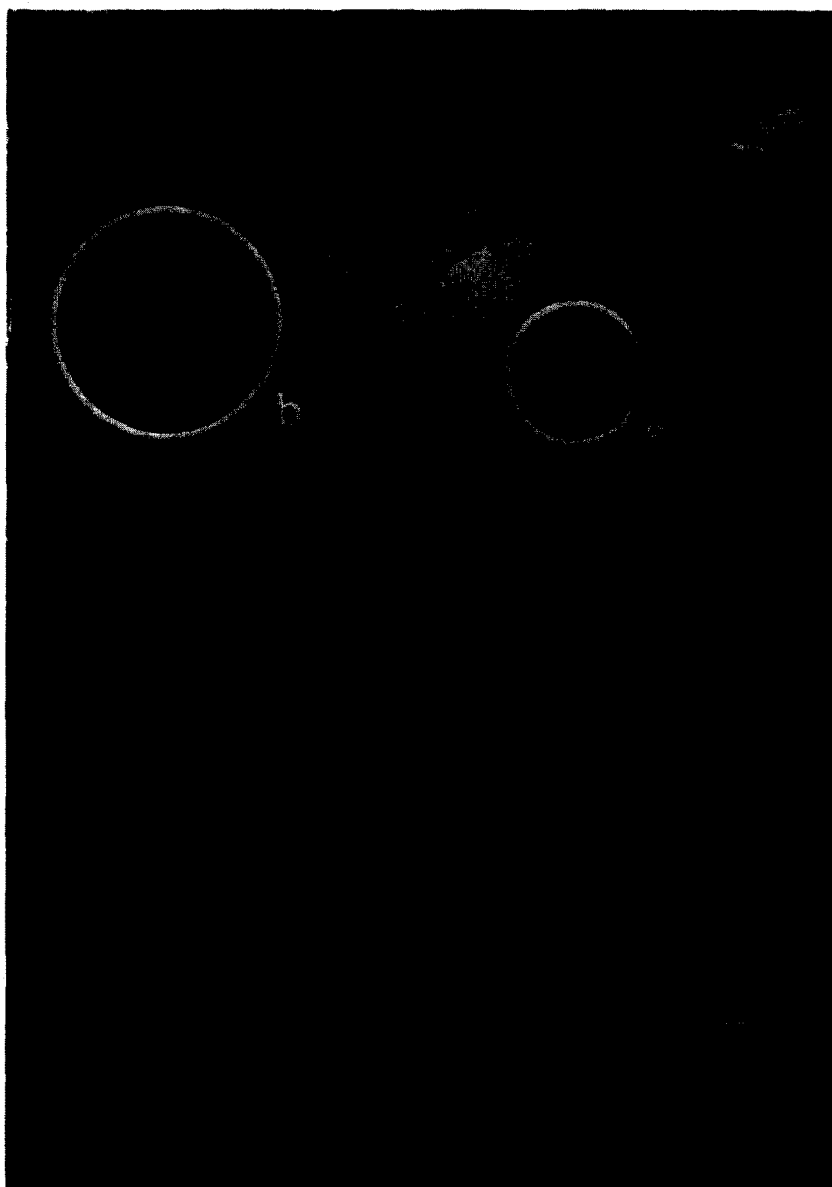


Fig. 5. Electromicrograph of a typical fracture surface from one of the specimens ( $\times 6000$ ).

**REFERENCES**

- [1] J. R. Rice, *Mechanics of crack tip deformation and extension by fatigue. Fatigue Crack Propagation, ASTM Spec. Tech. Publ. No. 415*, p. 247. Am. Soc. Testing Mater (1967).
- [2] W. Elber, *Fatigue crack propagation. Ph.D. Thesis, Univ. of N.S.W., Australia* (1968).

(Received 17 June 1969)

**Résumé**—On présente les résultats d'une recherche indiquant qu'une fissure due à la fatigue, se propageant sous une charge allant de zéro à la tension qui peut être partiellement ou complètement refermée à la charge zéro. Une analyse de la distribution de la tension agissant sur les surfaces de fracture, montre que les maxima de la force locale de compression, peuvent dépasser la tension limite du matériau. La preuve fractographique est présentée dans le but de montrer que la fermeture de la fissure peut influencer la forme du modèle de striation sur les surfaces de fracture.

**Zusammenfassung**—Es werden die Ergebnisse einer Untersuchung dargelegt, die daraufhindeuten, dass ein unter Ursprungsbelastung wachsender Ermüdungsbruch im unbelasteten Zustand teilweise oder ganz geschlossen sein kann. Eine Analyse der auf der Bruchfläche vorhandenen Spannungsverteilung zeigt, dass die örtlichen Druckspannungshöchstwerte die Fließgrenze des Werkstoffes übertreffen können. Es wird fraktographisches Beweismaterial geliefert um zu zeigen, dass ein Schliessen des Risses die Form des Markierungsmusters auf den Bruchflächen beeinflussen kann.